RSC Advances

PAPER

View Article Online
View Journal | View Issue

Cite this: *RSC Adv.*, 2026, **16**, 10080

Crystal phase formation in crowded lysozyme solutions

Ivaylo L. Dimitrov *[ab]

Lysozyme crystallization in a crowded environment is investigated. Buffered protein solutions at pH 4.0 are used with no added precipitant (*e.g.* sodium chloride). Lysozyme concentrations over 250 mg ml^{-1} and 0.31 M buffer salt (sodium acetate) are attained *via* equilibration of two microliter volume drops which possess different initial vapor pressure. The study demonstrates that gradual lysozyme crowding can lead to abrupt crystal phase formation by effective widening of the metastable zone and narrowing the nucleation zone towards the unstable region of the protein-salt phase diagram. The nucleation events occur perceivably in a cooperative manner. The crystal growth is rapid and finally the crystals occupy almost the whole drop volume. Virtually no temperature dependence of the crystal formation is observed in the interval 18–33 °C, except for the equilibration rate. The developed approach can be successfully used for adequate prediction of the time when crystal nucleation starts.

Received 5th November 2025
Accepted 26th January 2026

DOI: 10.1039/d5ra08505e

rsc.li/rsc-advances

Introduction

The vapor diffusion method[1] is one of the most common methods for crystallization of proteins. Usually, a small volume of protein-containing solution is deposited on a surface near a separately placed larger volume of precipitant (salt-rich) solution in a closed system. Because of the difference in their vapor pressure, water is transferred from the high vapor pressure phase (the protein-containing solution) to the low vapor pressure phase (the salt-rich solution) until an equilibrium is eventually achieved. Thus, the protein concentration rises along with the concentration of other solution compounds that are normally added to modify protein–protein interactions and the protein gradually enters in a region of the phase diagram, where the probability for crystal formation is expected to be high enough. The main advantage of the vapor diffusion method is the slow (*e.g.* days) concentrating of the protein in the protein-containing solution. Typically, this leads to mild conditions for crystallization and allows good control over the processes of crystal nucleation and growth. Most often the vapor diffusion method is used for routine screening experiments and typically involves mixing of equal volume parts[2] of a buffered protein solution and a chosen precipitant solution to compose the protein-containing solution before closing the system for equilibration. The precipitant represents a chemical substance that may significantly alter the protein solubility, and thus facilitates a transformation of the initially dissolved protein to another phase. If the precipitant concentration is too high, a relatively low protein concentration might be needed in order to bring the solution to the desired metastability. Conversely, if the precipitant concentration is too low, higher protein concentration would be needed for reaching the nucleation zone in the composition–composition phase diagram of the protein solution.[3]

There already have been successful attempts towards lysozyme crystallization by the batch method in solutions of very low ionic strength and practically zero precipitant concentration (sodium chloride (NaCl)).[4] A precipitant-free mode using either centrifugal concentration,[5] drying of highly concentrated lysozyme solutions containing 10 mM hydrochloric acid[6] or surface-induced crystallization of buffered lysozyme solutions at surprisingly low concentration[7,8] have been beneficially applied as well. Here we present an adaptable experimental approach that is based on the vapor-diffusion method, and reproducibly leads to impressive lysozyme crystal formation in buffered and crowded lysozyme solutions with no added NaCl – the most common precipitant for this protein. The approach could be relevant to studies which address the behavior of complex biological systems in a crowded environment, *e.g.* the cytosol.

Experimental section

Materials

The protein-containing solution was prepared by dissolving commercial lysozyme (chicken egg white from Sigma, 3X crystallized, dialyzed and lyophilized) in sodium acetate (NaAC) buffer with concentration 0.1 M and pH 4.0. The concentration of lysozyme stock solution was 80 mg ml^{-1}. The buffer solution

[a]*Institute of Physical Chemistry "Rostislaw Kaischew", Bulgarian Academy of Sciences, Acad. G. Bonchev Str., bl. 11, 1113 Sofia, Bulgaria. E-mail: idimitrov@ipc.bas.bg*
[b]*National Centre of Excellence Mechatronics and Clean Technologies, 8 bul. Kliment Ohridski, 1756 Sofia, Bulgaria*

was filtered through 0.22 μm filter to eliminate the potential presence of dust particles. The salt-rich solution was prepared by dissolving NaCl in the buffer solution. The concentration of NaCl stock solution was 0.85 M. It was also filtered through 0.22 μm filter. All solutions were stored at 4 °C.

Description of the approach

The protein-containing solution is deposited in the form of a small drop on a microscope cover glass. Near the protein-containing drop is deposited the salt-rich drop. Then the system is covered with a small glass lid, preliminary greased with Dow Corning high vacuum grease, and sealed to prevent evaporation of the drops outside the experimental system. This procedure takes less than 20 s. The system is left undisturbed. As time passes, the low vapor pressure drop (salt-rich drop) drains water from the high vapor pressure drop (protein-containing drop) until an equilibrium is eventually achieved when the two drops possess one and the same vapor pressure (Fig. 1).

Because the volume reserved for the vapor phase (the air volume under the glass lid) is small (2.15 cm^3), we can assume that the amount of water which remains retained in the vapor phase is inconsequential.[9] Also, because the volume of the drops falls in the microliter range, we can ignore the influence of the drop curvature on the vapor pressure too.[9] Being a colligative property, lowering of the water vapor pressure in relevant systems is driven by the dissolved salts and not by the dissolved protein, which is due to the much higher molar concentration of the low molecular weight substance as compared to that of the protein, even if the macromolecules are in crowded environment (hundreds of milligrams per milliliter[10]). For instance, 200 mg ml^{-1} lysozyme is expected to contribute less than 1.5% to the water vapor pressure lowering of a 0.85 M NaCl – the initial NaCl concentration in the salt-rich solution used in the present study.

Taking into account the above assumptions, we can make use of the following set of equations:

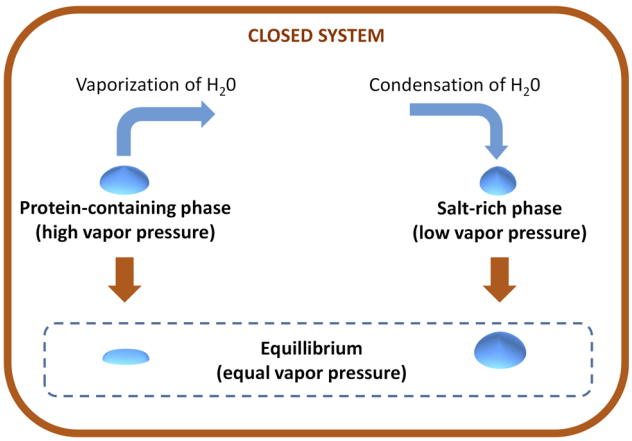

Fig. 1 Basic representation of the vapor diffusion method applied for two small (microliter) volume phases in a closed system. The high vapor pressure phase donates water to the low vapor pressure phase until equilibrium is achieved.

$$C_2 = (C_1 \times V_1 + C_3 \times V_3)/(V_1 + V_3) \quad (1)$$

$$V_2 = V_1 \times C_1/C_2 \quad (2)$$

$$V_1 + V_3 = V_2 + V_4 \quad (3)$$

$$V_4 = V_3 \times C_3/C_2 \quad (4)$$

where V_1 is the initial volume of the drop with the initial lower salt concentration (NaAC-buffered protein-containing drop), C_1 is the initial salt concentration of the drop with the initial lower salt concentration (NaAC-buffered protein-containing drop), V_2 is the equilibrium volume of the drop with the initial lower salt concentration (NaAC-buffered protein-containing drop), C_2 is the equilibrium salt concentration of the drop with the initial lower/higher salt concentration, V_3 is the initial volume of the drop with the initial higher salt concentration (NaCl salt-rich drop), C_3 is the initial salt concentration of the drop with the initial higher salt concentration (NaCl salt-rich drop), V_4 is the equilibrium volume of the drop with the initial higher salt concentration (NaCl salt-rich drop). (Because at equilibrium $C_2 = C_4$, C_4, the equilibrium salt concentration of the drop with the initial higher salt concentration, is omitted from consideration.)

With the help of these equations we can calculate the protein/salt equilibrium concentration and the equilibrium volume for arbitrary volume and protein/salt concentration of the initially deposited drops. Note that when the protein concentration rises in the protein-containing drop throughout the concentrating process, so does the buffer salt concentration in the same drop.

Experimental conditions

In order to test the proposed approach for concentrating protein solutions and to explore the possibilities for formation of a new phase, we investigated three set-ups, choosing the total liquid volume in the closed system to be 20 μL:

1. $V_1 = 5$ μL, $V_3 = 15$ μL.
2. $V_1 = 10$ μL, $V_3 = 10$ μL.
3. $V_1 = 15$ μL, $V_3 = 5$ μL.

Using eqn (1)–(4) with $C_1 = 0.1$ M (NaAC, 80 mg ml^{-1} lysozyme) and $C_3 = 0.95$ M (NaCl + NaAC), we obtain the following anticipated equilibrium values of concentration and volume for the each of the set-ups:

1. $C_2 = 0.74$ M salt (and 570 mg ml^{-1} lysozyme), $V_2 = 0.7$ μL, $V_4 = 19.3$ μL.
2. $C_2 = 0.53$ M salt (and 420 mg ml^{-1} lysozyme), $V_2 = 1.9$ μL, $V_4 = 18.1$ μL.
3. $C_2 = 0.31$ M salt (and 250 mg ml^{-1} lysozyme), $V_2 = 4.8$ μL, $V_4 = 15.2$ μL.

Hereinafter we shall use the following designation for the three set-ups, depending on the initial volume of the NaAC-buffered protein-containing drop, starting from the smallest one: *S*-configuration (5 μL initial volume of the NaAC-buffered protein-containing drop), *M*-configuration (10 μL initial volume of the NaAC-buffered protein-containing drop) and *L*-

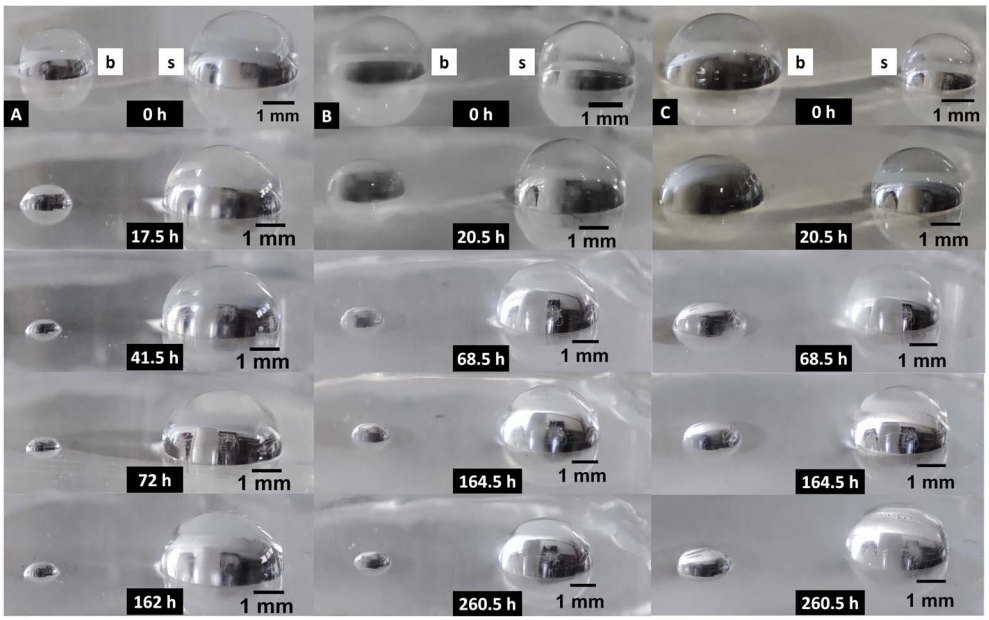

Fig. 2 Illustration of the experimental set-up. Equilibration of the salt-rich drop (s, 0.95 M) against the buffer drop (b, 0.1 M) in a closed system, representing the experimental set-up. Column A – *S*-configuration, column B – *M*-configuration, column C – *L*-configuration. The time that have passed since the deposition of the drops is shown in hours (h) for each configuration. The temperature is 23 ± 3 °C.

configuration (15 μL initial volume of the NaAC-buffered protein-containing drop), respectively.

The goals of the study require only approximate experimental validation of the calculated equilibrium data. Because the protein in the solution was expected eventually to undergo a phase transition upon concentrating, we tested if the system is airtight with a drop of the NaAC buffer (protein-free) equilibrating against the salt-rich drop (Fig. 2).

The experiments are performed at ambient temperature. It may vary up to several degrees in a single experiment and the entire covered interval during the study is 18–33 °C. For the aims of the current investigation – to demonstrate an approach for obtaining crowded protein solutions and to explore the conditions for triggering the formation of a solid phase in a highly reproducible manner – the temperature appears as a factor of relatively little importance (see below).

The experiments are performed on a hydrophobized microscope cover glass made of chemically resistant borosilicate glass D 263® M of the first hydrolytic class. This surface is selected because the drops remain well-shaped and the volume change can be easily detected. The only discovered drawback of the hydrophobic coverage is that the drops can easily slide across the surface and spoil the experiment. Furthermore, if a drop contains protein, it reshapes, because it preserves its diameter when its volume decreases. This observation is valid for both highly hydrophobic surface (the selected one) and low hydrophobic surface (non-hydrophobized borosilicate glass). Therefore, no adsorbed protein will be lost during drop evaporation.

Additional test trials made in the course of optimization of the experimental set-up show that (i) an eventual phase formation does not depend on the degree of hydrophobicity of the glass surface, (ii) the behavior of the protein solution does not depend on how freshly prepared the stock solutions are, (iii) the presence or absence of protein in the higher vapor pressure drop does not affect the time for reaching of equilibrium.

Results and discussion

The *S*-configuration appears most suitable to test how airtight the assembled system is, because it leads to a volume of the NaAC-buffered drop (protein-free), which falls in the nanoliter range. After the equilibration is achieved, the drop retains its volume (Fig. 2A). The drops might eventually evaporate in several months, but this observation is inconsequential to the present study. The new phase forms in a much shorter time frame as we will see below.

Since no temperature control was applied, temperature of the experiments varied from about 18 °C to about 33 °C for the duration of the study. It is important to note that even the water vapor pressure increases more than twice from 18 °C to about 33 °C, the liquid drop volume remains essentially the same,[9] and so does the concentration of the respective drop constituents. Different temperature values in this interval, however, effectively alter the time for reaching of the equilibrium, or basically the evaporation and condensation rates. Under used solutions' composition the time for reaching of the equilibrium is dependent also on the initial volume and surface of the salt-rich and protein-containing drops, and falls in the range 24–168 hours for the different experimental configurations. Still, the main transfer of water through the vapor phase occurs roughly during the first 20–30 hours for *S*- and *M*-configurations, and 2–3 days for *L*-configuration (empirical evidence, *e.g.* Fig. 2). During this transfer, >90% of the water volume, that is expected to be transferred throughout the process, is transferred. That means at least 3.9 μL of water for *S*-configuration (4.3 μL full transfer at equilibrium), at least 7.3 μL of water for *M*-

configuration (8.1 μL full transfer at equilibrium), and at least 9.2 μL of water for *L*-configuration (10.2 μL full transfer at equilibrium). The time of transfer is represented by interval of values, because the rate at which the protein-containing drop concentrates is dependent on temperature. It should be emphasized here, that the rate of drops' equilibration will decelerate considerably when the vapor pressure difference of the drops becomes smaller and smaller. This fact justifies the pragmatic focus on the main transfer of water. Note also that the size bars are intentionally present on each of the images, because every image was processed individually, and the images must not be just compared to one another.

Upon concentrating the protein-containing drop, we found that the protein reproducibly crystallizes (Fig. 3). It is worth noting that no other types of phase formation (*e.g.* amorphous precipitation, liquid–liquid phase separation) were observed in the present investigation.

An important observation in this study is that the crystallization outcome is basically the same across all of the used configurations (Fig. 4). The NaAC-buffered crowded lysozyme solutions crystallize in the tetragonal form (Fig. 3 and 4) in the absence of added NaCl even at temperature above 30 °C, where the orthorhombic crystal form is normally expected to develop.[11]

The crystallization process exhibits remarkable reproducibility among all individual experiments for each of the configurations, both in time and crystallization outcome. That reproducibility leads to the opportunity of successfully forecasting the time of crystallization and allows investigation of the nucleation onset and the subsequent crystal growth (study in progress). The higher is the final concentration of lysozyme in the protein-containing drop, the higher is the probability for proper timing and capturing of the initial stages of the new phase formation.

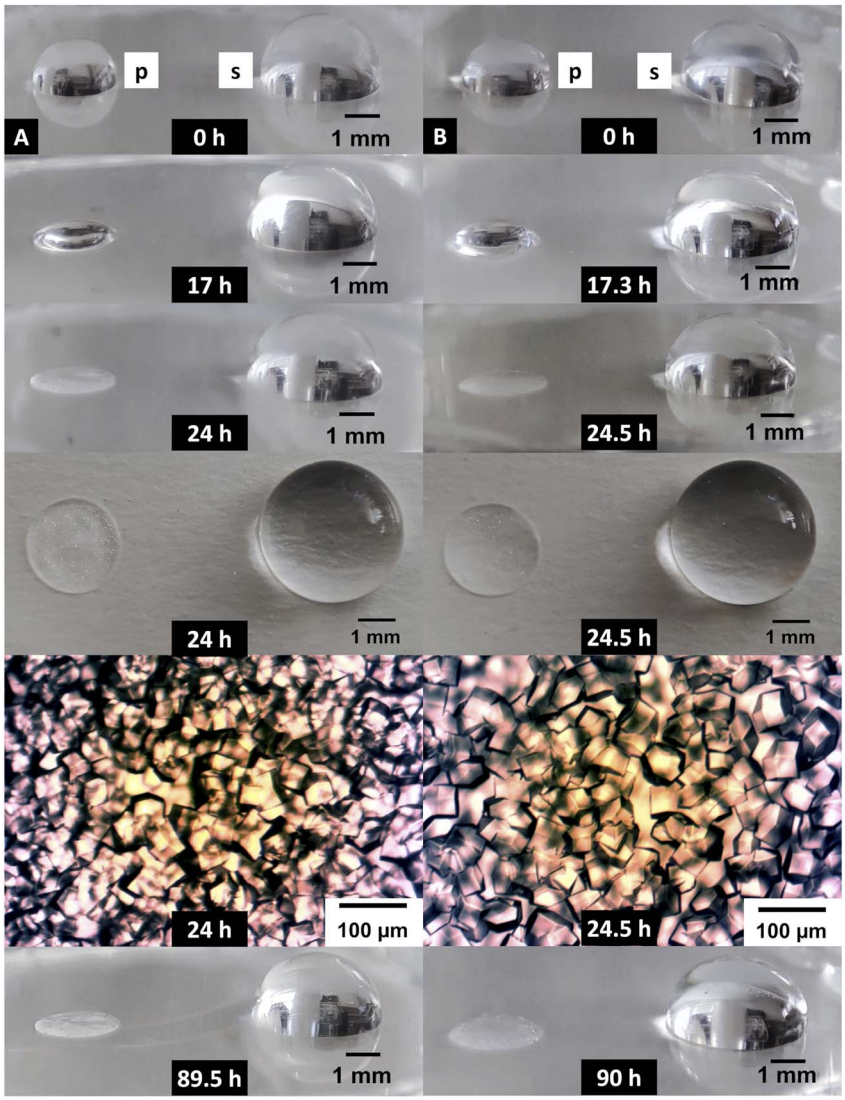

Fig. 3 Equilibration of the salt-rich drop (s, 0.95 M) against the protein-containing drop (p, ≈ 0.1 M) in *S*-configuration. Column A and column B represent separate experiments. The time that have passed since the deposition of the drops is shown in hours (h). The temperature of A is 22 ± 2 °C. The temperature of B is 21 ± 3 °C. The nucleation starts around the 20th hour of equilibration. Some of the images show that the crystallization can be easily detected even macroscopically. An example of a top view is also shown.

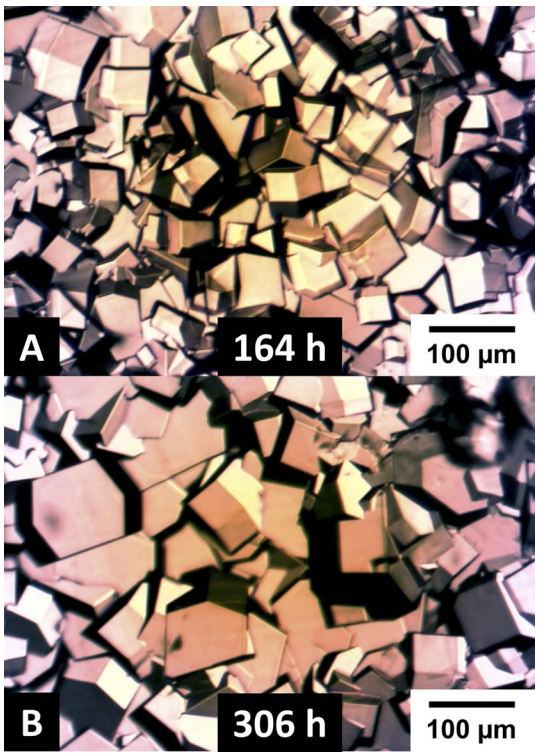

Fig. 4 Representative images of the lysozyme crystal population in *M*-configuration (A), and *L*-configuration (B). The time that have passed since the deposition of the drops is shown in hours (h). The temperature of A and B is 23 ± 3 °C. The nucleation in A starts around the 42nd hour of equilibration. The nucleation in B starts around the 192nd hour of equilibration.

It is not necessary for the system to attain equilibrium for the nucleation to start. Depending on the experimental conditions (*e.g.* lysozyme/salt concentration, volume of drops), the nucleation could be triggered before equilibrium is attained, but certainly a particular lysozyme solution composition is required for the process to start. Because the nucleation and the subsequent crystal growth could lead to a volume change in the protein-containing drop and a change in the solution composition, the equilibrium cannot be precisely estimated. Therefore, it would be more adequate if we speak of a quasi-equilibrium in the case of *S*-configuration and likely in the case of *M*-configuration. Because the protein-containing drop in *L*-configuration does not nucleate for a period that is longer than the time needed for attaining of the quasi-equilibrium (3–4 days for the lowest values of temperature), we can say that the equilibrium protein/salt concentration in this configuration is the limit at which the nucleation occurs. This limit is 250 mg ml^{-1} lysozyme and 0.31 M salt.

It is shown that lysozyme solubility rises in NaAC above 0.1 M at pH 4.0,[12] but decrease again at higher NaAC concentration, *e.g.* 0.5 M, the percentage effect of the buffer concentration on the lysozyme solubility being less pronounced at descending NaCl concentration. Therefore, we can suggest that it is the high concentration of the protein[4] that is predominantly responsible for the very phase transition. On one hand, this suggestion is supported by the unusually abrupt onset of nucleation, when there is essentially constant and moderate NaAC concentration, that is not expected to lead in any way to a sharp decrease of the protein solubility. On the other hand, the above suggestion is made on the basis of investigated lysozyme solutions that contain both NaAC and NaCl, and the assumed irrelevance of the NaAC concentration might appear inadequate. Note also, that in the absence or low concentration (up to 0.1 M) of NaCl the lysozyme supersaturation ratio at pH 4.0 is shown to be small (up to 1.5), but could increase several times (up to 7.3) upon rising the concentration (up to 1.2 M) of this strong precipitant for lysozyme.[4] In 0.1 M NaAC and pH 4.0, like in the case under consideration, rising NaCl concentration only 3.5 times can reduce the solubility of lysozyme as much as 30 times.[12] All that suggest complex interplay between the protein and different salt ions.

It is known that lysozyme is very soluble in 0.1 M NaAC, pH 4.0, and small NaCl concentration (less than 0.2 M) even at temperature around 12 °C.[13] Based on the uncommon results of the present study, we suggest that salting-in effect (lysozyme becomes more soluble) takes place initially with the increase of NaAC buffer concentration beyond 0.1 M during the decrease in volume of the protein-containing drop. This increase is accompanied with increase in the lysozyme concentration, gradually driving the solution to metastability. Then, at some buffer concentration, most likely around 0.3 M, a salting-out effect (lysozyme becomes less soluble) begins to dominate the solution behavior, adding to the effect of the accretive crowding of the protein if the equilibrium in the experimental system is still not achieved. These two effects (the salting-out effect and the crowding effect) transfer the system to the labile, nucleation zone, where the nucleation process unfolds quickly. However, we might also have witnessed an effective widening of the zone where the protein solution cannot nucleate in a reasonable time frame (a.k.a. metastable zone), and hence narrowing of the nucleation zone. Probably, the crowding effect, facilitated by the initial salting-in effect, results in restricted motion of the protein molecules, thus providing for "nucleation-free metastability" (*e.g.* the alignment of the protein surface patches, needed for the formation of crystal contacts, is rendered difficult). Moreover, we can see that most of the lysozyme in the protein-containing drops turns into crystal (Fig. 3 and 4), which testifies for low solubility. That means NaAC could really appear to be a good salting-out agent at a moderate concentration (*e.g.* 0.3–0.7 M). A representation of our hypothesis is shown in Fig. 5.

Note that depending on the initial solution composition and other experimental parameters, the white dashed single arrow in Fig. 5 can be of different length and situated anywhere across the phase diagram, but for a vapor diffusion approach it makes sense only if it begins in the stable or the metastable region. Also, it must reflect the equal rise of concentration for all of the solution constituents. Besides the importance of the initial solution composition, of significance would also be the rate at which the solution concentrates, possibly leading to variety of kinetic effects. The concentration path, traced by the white dashed single arrow in Fig. 5, is an illustration of the change in

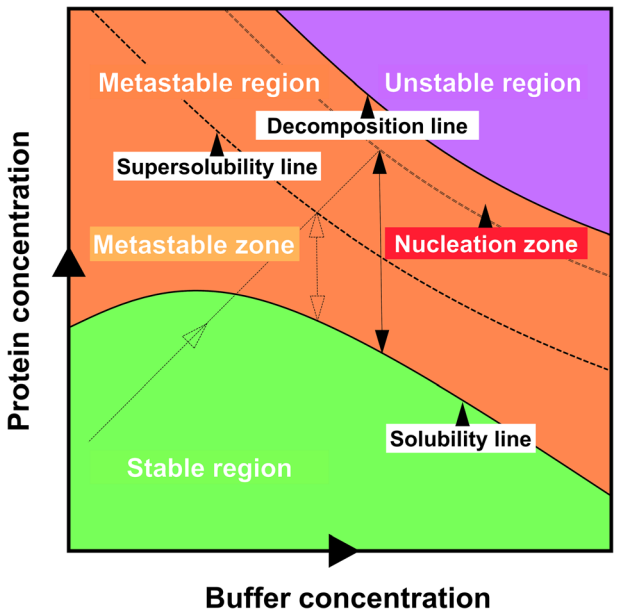

Fig. 5 Visualization of the hypothesis, discussed in the text. The scheme shows the structure of a common protein-salt (composition–composition type) phase diagram. The salting-in effect is represented by a solubility line that exhibits a maximum. The supersolubility line (dashed line) is an imaginary line that divides the metastable region into two parts – metastable zone and nucleation zone. This division is artificial and is made from experimental perspective. The metastable zone is the zone where no crystals will be observed, although the solution is supersaturated. The nucleation zone is the zone where crystals will eventually be observed in the timeframe of the experiment. The metastable and the unstable regions are divided by the decomposition line. In the unstable region a protein-rich and protein-depleted phases appear spontaneously. Transparent dashed double arrow shows the initial width of the metastable zone. Black solid double arrow shows widening of the metastable zone through displacement of the supersolubility curve toward the decomposition line and thus narrowing the nucleation zone. The double dashed line marks the new position of the supersolubility line, and the label "nucleation zone" in the figure points to the new, narrowed nucleation zone. Both double arrows, measuring the width of the metastable zone, are vertical under the assumption that only the protein concentration changes in the initial phase after the protein crystal nucleation and growth. Transparent dashed single arrow shows an example of the path of concentrating the initial phase in a vapor diffusion set-up.

solution composition in our experimental set-up. The direction of this path is one and the same for *S*-configuration, *M*-configuration, and *L*-configuration. However, the rate of solution concentration under the applied experimental conditions is different, and such would be the length of the concentration path. Due to kinetic phenomena (*e.g.* restricted diffusion of the protein molecules in crowded environment), a higher rate of solution concentration may place the solution even deeper in the nucleation zone before initiation of the crystallization. Hence, very high probability for nucleation could be achieved. This would effectively make the metastable zone even wider (imagine a longer black solid double arrow (Fig. 5) that is shifted to the right). As already mentioned earlier, the nucleation is not necessarily triggered at equilibrium. For *S*-configuration the nucleation process will takes place somewhere between 250 and 570 mg ml^{-1} lysozyme, and the respective buffer concentration between 0.31 and 0.74 M. This situation would result in the highest nucleation rate, which is manifested by the highest number of smallest crystals (Fig. 3, roughly 50 μm average crystal length). Accordingly, larger crystals of lower number are observed for the less concentrated (nucleation occurs in the concentration range 250–420 mg ml^{-1} lysozyme, 0.31–0.53 M NaAC) solution in *M*-configuration (Fig. 4A, roughly 75 μm average crystal length), and largest crystals of lowest number for least concentrated ($\approx$250 mg ml^{-1} lysozyme, $\approx$ 0.31 M NaAC) *L*-configuration (Fig. 4B, roughly 100 μm average crystal length).

The proposed effective displacement of the supersolubility curve toward the decomposition line means that the nucleation zone can be described as a zone of very high probability for nucleation. That is why we observe an abrupt onset of crystal nucleation after a certain solution composition is established. Although a decomposition into ordered solid phase seems not reasonable,[3] it is worth mentioning that if the protein-containing drop is inspected for the first time 24–30 hours after the beginning of the experiment, the complete phase transformation in *S*-configuration could be mistaken for manifestation of a spinodal decomposition – virtually all of the drop volume turns into a population of relatively small crystals (*e.g.* Fig. 3). An example of the behavior of lysozyme solutions in the unstable region of a phase diagram can be found elsewhere.[14]

As noted above, 250 mg ml^{-1} lysozyme in 0.31 M NaAC buffer at pH 4 is estimated as particular solution composition for nucleation of lysozyme crystals (*L*-configuration). Because both lysozyme and NaAC concentration values are practically invariable at equilibrium, the crystal phase formation could still be influenced by fluctuations in temperature. The nucleation and crystal growth occur in a relatively short time frame even in *L*-configuration (up to few hours for nucleation and up to few days for crystal growth) compared to the time needed for the drop to nucleate (around 8–9 days at a lower temperature interval (18–26 °C), and around 3–4 days at a higher temperature interval (28–33 °C)). And this time is longer than the time needed for the quasi-equilibrium to be achieved for each of the temperature intervals. We remind that the *L*-configuration defines the mildest nucleation condition in the present study, and the particular one that clearly exhibits temperature dependence of the nucleation, but only with respect to the equilibration time, and hence to the rate of equilibration. The effect of temperature on the crystallization kinetics is expected to be similar across used configurations, leading to accelerated crystal growth at higher temperatures. Because we can find in the literature no evidence for inverse temperature dependence of the lysozyme solubility,[15] such issue is not considered here.

The isoelectric point (pI) of lysozyme is close to 11.[16] Accordingly, at pH 4 the net charge of lysozyme is strongly positive and the interaction between protein molecules is repulsive. Increasing the ionic strength of a solution reverses this behavior and the interaction becomes attractive.[17] Although for lysozyme the salting-out anions are known to obey a reversed

Hoffmeister series, the chloride anion appearing to be the stronger precipitation anion,[18] acetate anion could also be powerful precipitant when its concentration rises beyond certain limit, as suggested above. However, the very high protein concentration could be even more important and we also should not exclude a possible synergistic effect.

The molecular crowding of lysozyme with effective radius of 17 Angstroms[18] would result in a volume fraction of 0.22 for the lysozyme in *L*-configuration and 0.51 for the lysozyme in *S*-configuration (on the condition that the equilibrium is reached before the nucleation onset). Sticking to the spherical approximation, the former value would roughly correspond to mean distance between lysozyme molecules which is 2/3 of the molecular diameter. The second value, respectively, is pretty close to the relatively loose sphere packing in the simple cubic lattice (0.52).[19] Such very close proximity is probably of crucial importance for the nucleation-related processes in our experimental system. Translational and especially rotational diffusivity could drop significantly along with an increase in viscosity at high values of protein volume fraction.[20] That might slow down patch–patch recognition and the alignment of protein molecules in the process of formation of crystal contacts, already proposed as a reason for the presumed "nucleation-free metastability" (see above). The effects of excluded volume or other crowding-related effects[21] could also be important in the case under consideration.

It has been proposed that there is a formation of a weakly specific complex in the protein–protein association, followed by a precise molecular docking.[22] Similar processes might also be involved in protein crystallization.[4] Alike two-stage behavior may be relevant to the protein solution behavior in our study, potentially explaining the observed nucleation in a very small time frame (*e.g.* several minutes for *S*-configuration) and in presumable cooperative manner (each single nucleation event seems like "facilitated" by the preceding nucleation event). This cooperative effect could be connected to local changes of density in the crowded environment that lead to successful protein–protein crystal association *via* molecular rearrangement.

Conclusion

In the present study we demonstrate a vapor diffusion method for concentrating buffered protein solution in three particular configurations, represented by different initial volumes of a protein-containing drop and a salt-rich drop equilibrating against each other. We found that nucleation of tetragonal lysozyme crystals can be triggered in crowded solutions that contain approximately 250 mg ml^{-1} and 0.3 M NaAC at pH 4. Even for this solution composition, which is the least concentrated among the used configurations, the nucleation is abrupt and intensive. We propose that the protein concentrating process is accompanied with effective displacement of the supersolubility curve toward the decomposition line in the protein-salt phase diagram. This leads to widening of the metastable zone and narrowing of the nucleation zone, gradually bringing the experimental solutions to a crowded environment, where the nucleation probability appears to be unusually high. A possible nucleation cooperative effect is guessed, which could be driven by local density changes that may stimulate protein molecules readily to rearrange and form crystal contacts. The temperature mainly controls the rate of reaching equilibrium. The demonstrated method ensures remarkable reproducibility both in time and crystallization outcome and allows successful forecasting of the nucleation onset, which is particularly difficult for stochastic processes like nucleation.

Conflicts of interest

There are no conflicts to declare.

Data availability

The data supporting this article have been included as part of the manuscript.

Acknowledgements

This work was supported by European Regional Development Fund under "Research Innovation and Digitization for Smart Transformation" program 2021-2027 under the Project BG16RFPR002-1.014-0006 "National Centre of Excellence Mechatronics and Clean Technologies". Equipment of the distributed research infrastructure INFRAMAT (National Roadmap for Scientific Infrastructure) supported by Bulgarian Ministry of Education and Science was used in these studies.

References

1 A. McPherson and J. A. Gavira, Introduction to protein crystallization, *Acta Crystallogr., Sect. F:Struct. Biol. Commun.*, 2014, **70**, 2–20, DOI: 10.1107/S2053230X13033141.
2 E. L. Forsythe, D. L. Maxwell and M. Pusey, Vapor diffusion, nucleation rates and the reservoir to crystallization volume ratio, *Acta Crystallogr., Sect. D:Biol. Crystallogr.*, 2002, **58**, 1601–1605, DOI: 10.1107/s0907444902014208.
3 B. Rupp, Origin and use of crystallization phase diagrams, *Acta Crystallogr., Sect. F:Struct. Biol. Commun.*, 2015, **71**, 247–260, DOI: 10.1107/S2053230X1500374X.
4 P. Retailleau, M. Riès-Kautt and A. Ducruix, No salting-in of lysozyme chloride observed at low ionic strength over a large range of pH, *Biophys. J.*, 1997, **73**, 2156–2163, DOI: 10.1016/S0006-3495(97)78246-8.
5 Y. Suzuki, H. Tsuge, H. Hondoh, Y. Kato, Y. Uehara, N. Maita, K. Hosokawa and S. Ueta, Precipitant-free lysozyme crystals grown by centrifugal concentration reveal structural changes, *Cryst. Growth Des.*, 2018, **18**, 4226–4229, DOI: 10.1021/acs.cgd.8b00326.
6 Y. Suzuki, S. Fujiwara, S. Ueta and T. Sakai, Precipitant-free crystallization of lysozyme and glucose isomerase by drying, *Crystals*, 2022, **12**, 129, DOI: 10.3390/cryst12020129.
7 A. S. Ghatak and A. Ghatak, Precipitantless crystallization of protein molecules induced by high surface potential, *Cryst.*

Growth Des., 2016, **16**, 5323–5329, DOI: 10.1021/acs.cgd.6b00833.

8 A. S. Ghatak, G. Rawal and A. Ghatak, Precipitant-free crystallization of protein molecules induced by incision on substrate, *Crystals*, 2017, **7**, 245, DOI: 10.3390/cryst7080245.

9 I. L. Dimitrov, Narrow size distribution of lysozyme crystals in a reverse vapor diffusion set-up, *CrystEngComm*, 2023, **25**, 1471–1478, DOI: 10.1039/D2CE01510B.

10 I. M. Kuznetsova, K. K. Turoverov and V. N. Uversky, What macromolecular crowding can do to a protein, *Int. J. Mol. Sci.*, 2014, **15**, 23090–23140, DOI: 10.3390/ijms151223090.

11 F. Ewing, E. Forsythe and M. Pusey, Orthorhombic lysozyme solubility, *Acta Crystallogr., Sect. D:Biol. Crystallogr.*, 1994, **50**, 424–428, DOI: 10.1107/S0907444993014428.

12 E. L. Forsythe and M. L. Pusey, The effects of acetate buffer concentration on lysozyme solubility, *J. Cryst. Growth*, 1996, **168**, 112–117, DOI: 10.1016/0022-0248(96)00368-5.

13 E. L. Forsythe, R. A. Judge and M. L. Pusey, Tetragonal chicken egg white lysozyme solubility in sodium chloride solutions, *J. Chem. Eng. Data*, 1999, **44**, 637–640, DOI: 10.1021/je980316a.

14 F. Cardinaux, T. Gibaud, A. Stradner and P. Schurtenberger, Interplay between spinodal decomposition and glass formation in proteins exhibiting short-range attractions, *Phys. Rev. Lett.*, 2007, **99**, 118301, DOI: 10.1103/PhysRevLett.99.118301.

15 J. P. Guilloteau, M. M. Riès-Kautt and A. F. Ducruix, Variation of lysozyme solubility as a function of temperature in the presence of organic and inorganic salts, *J. Cryst. Growth*, 1992, **122**, 223–230, DOI: 10.1016/0022-0248(92)90249-I.

16 S. Jalili-Firoozinezhad, M. Filippi, F. Mohabatpour, D. Letourneur and A. Scherberich, Chicken egg white: hatching of a new old biomaterial, *Mater. Today*, 2020, **40**, 193–214, DOI: 10.1016/j.mattod.2020.05.022.

17 A. Ducruix, J. P. Guilloteau, M. Riès-Kautt and A. Tardieu, Protein interactions as seen by solution X-ray scattering prior to crystallogenesis, *J. Cryst. Growth*, 1996, **168**, 28–39, DOI: 10.1016/0022-0248(96)00359-4.

18 A. A. Chernov and H. Komatsu, Principles of crystal growth in protein crystallization, in *Science and Technology of Crystal Growth*, ed. J. P. van der Eerden and O. S. L. Bruinsma, Springer, Dordrecht, 1995, pp. 329–353, DOI: 10.1007/978-94-011-0137-0_24.

19 I. Martin, B. Dozin, R. Quarto, R. Cancedda and F. Beltrame, Computer-based technique for cell aggregation analysis and cell aggregation in *in vitro* chondrogenesis, *Cytometry*, 1997, **28**, 141–146, DOI: 10.1002/(sici)1097-0320(19970601)28:2<141::aid-cyto7>3.0.co;2-i.

20 Z. Bashardanesh, J. Elf, H. Zhang and D. van der Spoel, Rotational and translational diffusion of proteins as a function of concentration, *ACS Omega*, 2019, **4**, 20654–20664, DOI: 10.1021/acsomega.9b02835.

21 A. C. Miklos, C. Li, N. G. Sharaf and G. J. Pielak, Volume exclusion and soft interaction effects on protein stability under crowded conditions, *Biochemistry*, 2010, **49**, 6984–6991, DOI: 10.1021/bi100727y.

22 G. Schreiber and A. R. Fersht, Rapid, electrostatically assisted association of proteins, *Nat. Struct. Biol.*, 1996, **3**, 427–431, DOI: 10.1038/nsb0596-427.